The author is grateful to Mr A. J. Hruza of Ferro Corp. (Australia) for synthesizing the sample, to Messrs G. L. Corino and I. C. Madsen of the CSIRO Division of Mineral Chemistry for assistance with the collection of the thermo-analytical and X-ray diffraction data, respectively, and to Mr N. Brown of the Central Resource Laboratory, University of Tasmania for the FTIR measurements. The Australian Associated Smelters Pty Ltd is also thanked for financial assistance and permission to publish the results.

References

ABEL, E. W. (1973). *Lead*. In *Comprehensive Inorganic Chemistry*, pp. 105–146. Oxford: Pergamon Press.

ANDERSON, J. S. & STERNS, M. (1959). *J. Inorg. Nucl. Chem.* **11**, 272–285.

BRAGG, L. & CLARINGBULL, G. F. (1965). *Crystal Structures of Minerals*. London: Bell & Sons.

BROWN, I. D. & WU, K. K. (1976). *Acta Cryst.* B**32**, 1957–1959.

BYSTRÖM, A. (1945). *Ark. Kemi Mineral. Geol.* **20**A, 1–31.

CAULDER, S. M., MURDAY, J. S. & SIMON, A. C. (1973). *J. Electrochem. Soc.* **120**, 1515–1516.

CHIARI, G. & FERRARIS, G. (1982). *Acta Cryst.* B**38**, 2331–2341.

CLARK, G. L. & TYLER, W. P. (1939). *J. Am. Chem. Soc.* **61**, 58–65.

DICKENS, B. (1965). *J. Inorg. Nucl. Chem.* **27**, 1495–1501.

GLEMSER, O. & LIN, T.-P. (1971). *Z. Anorg. Allg. Chem.* **382**, 244–248.

HEWAT, A. W. (1979). *Acta Cryst.* A**35**, 248.

HILL, R. J. (1982). *Mater. Res. Bull.* **17**, 769–784.

HILL, R. J. (1984). *J. Power Sources*, **11**, 19–32.

HILL, R. J. & HOUCHIN, M. R. (1985). *Electrochim. Acta*, **30**. In the press.

HILL, R. J. & HOWARD, C. J. (1985). *J. Appl. Cryst.* **18**, 173–180.

HILL, R. J., JESSEL, A. M. & MADSEN, I. C. (1985). Proc. Lead-acid Battery Symposium, 166th Meeting of the Electrochem. Soc., New Orleans, 7–11 October.

HILL, R. J. & MADSEN, I. C. (1984). *J. Electrochem. Soc.* **131**, 1486–1491.

HOWARD, C. J., BALL, C. J., DAVIS, R. L. & ELCOMBE, M. M. (1983). *Aust. J. Phys.* **36**, 507–518.

HOWIE, R. A. & MOSER, W. (1968). *Nature* (*London*), **219**, 372–373.

International Tables for X-ray Crystallography (1974). Vol. IV. Birmingham: Kynoch Press. (Present distributor D. Reidel, Dordrecht.)

MORANO, R. T. (1978). *Thermochim. Acta*, **26**, 27–37.

OSWALD, H. R., GUNTER, J. R. & STAHLIN, W. (1968). *Helv. Chim. Acta*, **51**, 1389–1394.

ROBIN, J. & THÉOLIER, A. (1956). *Bull. Soc. Chim. Fr.* pp. 680–681.

SAHL, K. (1970). *Lead*. In *Handbook of Geochemistry*, pp. 82A1–6. Berlin: Springer-Verlag.

TODD, G. & PARRY, E. (1964). *Nature* (*London*), **202**, 386–387.

TOLKACHEV, S. S., STROGANOV, E. V. & KOZINA, I. I. (1958). *Vestn. Leningr. Univ.* **16**, 134–139.

WILES, D. B. & YOUNG, R. A. (1981). *J. Appl. Cryst.* **14**, 149–151.

YOUNG, R. A., PRINCE, E. & SPARKS, R. A. (1982). *J. Appl. Cryst.* **15**, 357–359.

Acta Cryst. (1985). C**41**, 1003–1007

Structure of High-Pressure Phases of Barium Germanium Oxide, $BaGe_2O_5$

BY MITUKO OZIMA

Institute for Solid State Physics, University of Tokyo, Roppongi, Minato-ku, Tokyo 106, *Japan*

(*Received* 2 *February* 1985; *accepted* 11 *March* 1985)

Abstract. (i) $BaGe_2O_5$ II: $M_r = 362{\cdot}56$, monoclinic, $P2_1/a$, $a = 13{\cdot}214\ (2)$, $b = 13{\cdot}043\ (2)$, $c = 9{\cdot}5501\ (8)$ Å, $\beta = 94{\cdot}006\ (10)°$, $V = 1642{\cdot}0\ (4)$ Å^3, $Z = 16$, $D_x = 5{\cdot}86$ g cm^{-3}, Ag $K\alpha$, $\lambda = 0{\cdot}56087$ Å, $\mu = 130{\cdot}9$ cm^{-1}, $F(000) = 2560$, $T = 300$ K, $R = 0{\cdot}047$ for 2549 independent reflections. (ii) $BaGe_2O_5$ III: orthorhombic, $Cmca$, $a = 5{\cdot}5632\ (2)$, $b = 9{\cdot}8711\ (6)$, $c = 14{\cdot}3231\ (12)$ Å, $V = 786{\cdot}56\ (10)$ Å^3, $Z = 8$, $D_x = 6{\cdot}12$ g cm^{-3}, Ag $K\alpha$, $\mu = 136{\cdot}7$ cm^{-1}, $F(000) = 1280$, $T = 300$ K, $R = 0{\cdot}051$ for 535 independent reflections. $BaGe_2O_5$ II (low-pressure and high-temperature phase) has three kinds of infinite chains of Ge polyhedra. One type (which is parallel to the b axis) is connected to another chain of the same type by the other two chains (which are parallel to the a axis) and two ladder-like sheets parallel to (201) and $(\bar{2}01)$, respectively, are formed. $BaGe_2O_5$ III (high-pressure and low-temperature phase) has a sheet structure similar to that for the hexagonal perovskite-like compounds ABX_3 at high pressures. The increase in coordination number of Ba from $BaGe_2O_5$ II to $BaGe_2O_5$ III is accompanied by a large increase in density (4·4%).

Introduction. $BaSi_2O_5$ is known as the mineral sanbornite, which belongs to orthorhombic space group $Pmnb$ with cell dimensions $a = 7{\cdot}6922\ (8)$, $b = 13{\cdot}525\ (1)$, $c = 4{\cdot}6336\ (5)$ Å [*Natl Bur. Stand.* (*US*) *Monogr.*, 1976], which has a monoclinic high-temperature modification with $C2/c$, $a = 23{\cdot}202\ (5)$, $b = 4{\cdot}661\ (1)$, $c = 13{\cdot}613\ (4)$ Å, $\beta = 97{\cdot}54\ (2)°$ (Katscher, Bissert & Liebau, 1973) at atmospheric pressure. Both have undulating sheet structures which consist of Ge tetrahedra.

0108-2701/85/071003-05$01.50

Germanates are frequently used as convenient high-pressure model substances for the corresponding silicate on account of their lower transition pressure. Ozima, Susaki, Akimoto & Shimizu (1982) have reported that $BaGe_2O_5$ I has two high-pressure phases ($BaGe_2O_5$ II and $BaGe_2O_5$ III) at 40–60 kbar (4–6 GPa). Further, they determined the boundary of these two phases, $P(\text{kbar}) = 7{\cdot}7 + 0{\cdot}047\,T(°\text{C})$, where $BaGe_2O_5$ II is the low-pressure high-temperature phase, and $BaGe_2O_5$ III is the high-pressure low-temperature phase. This implies that sunbornite transforms similarly at high pressures. Ozima *et al.* (1982) could not obtain single crystals of $BaGe_2O_5$ III and, accordingly, on the basis of the powder diffraction pattern, tetragonal symmetry was suggested. Recently, Kobayashi, Ozima, Shimizu & Akimoto (1983) have succeeded in obtaining single crystals of $BaGe_2O_5$ III and have revealed that this has orthorhombic symmetry.

In this paper, structures of both $BaGe_2O_5$ II and $BaGe_2O_5$ III are reported.

Table 1. *Fractional coordinates* ($\times 10^5$ *for* Ba, Ge; $\times 10^4$ *for* O) *and equivalent isotropic thermal parameters* ($\times 10^2$) *with e.s.d.'s in parentheses for* $BaGe_2O_5$ II *and* $BaGe_2O_5$ III

$$B_{\rm eq} = \tfrac{8}{3}\pi^2 \textstyle\sum_i \sum_j U_{ij} a_i^* a_j^* \mathbf{a}_i.\mathbf{a}_j.$$

	x	y	z	$B_{\rm eq}$(Å^2)
(i) $BaGe_2O_5$ II				
Ba(1)	36510 (8)	24609 (9)	12029 (11)	75 (2)
Ba(2)	11639 (8)	25350 (9)	86057 (12)	95 (2)
Ba(3)	36797 (9)	1425 (9)	38873 (12)	79 (2)
Ba(4)	13140 (9)	1010 (9)	61294 (12)	74 (2)
Ge(1)	26382 (14)	−9 (16)	−1332 (20)	70 (4)
Ge(2)	−1704 (13)	24548 (15)	47310 (17)	52 (4)
Ge(3)	0	50000	0	51 (5)
Ge(4)	9097 (14)	12965 (15)	23891 (19)	52 (4)
Ge(5)	12009 (14)	36683 (16)	23994 (20)	60 (4)
Ge(6)	39116 (14)	15099 (15)	73474 (19)	55 (4)
Ge(7)	38531 (15)	39238 (15)	74828 (21)	70 (4)
Ge(8)	23835 (13)	27384 (15)	51635 (18)	59 (4)
Ge(9)	0	0	0	293 (11)
O(1)	360 (9)	1245 (10)	656 (13)	53 (26)
O(2)	354 (10)	3705 (10)	675 (15)	101 (30)
O(3)	−181 (9)	1494 (9)	3280 (13)	52 (25)
O(4)	77 (11)	3483 (11)	3357 (15)	129 (32)
O(5)	1668 (10)	2389 (10)	2199 (13)	100 (28)
O(6)	1609 (10)	274 (11)	3074 (14)	96 (29)
O(7)	1964 (9)	3908 (10)	4144 (14)	76 (28)
O(8)	2329 (10)	4175 (11)	1595 (14)	100 (30)
O(9)	3730 (9)	−74 (12)	1024 (13)	95 (29)
O(10)	3416 (9)	2322 (12)	4198 (13)	101 (29)
O(11)	4874 (10)	1525 (10)	6122 (13)	81 (28)
O(12)	4478 (9)	3661 (10)	5856 (14)	78 (27)
O(13)	5085 (9)	4489 (10)	8231 (12)	44 (25)
O(14)	4110 (10)	2641 (11)	8349 (14)	103 (29)
O(15)	4286 (9)	435 (11)	8295 (13)	87 (28)
O(16)	3422 (13)	4373 (14)	9439 (16)	225 (41)
O(17)	2417 (11)	1266 (12)	−534 (18)	186 (37)
O(18)	2771 (11)	1399 (11)	6333 (15)	121 (31)
O(19)	2587 (11)	3467 (11)	6775 (13)	112 (31)
O(20)	1212 (9)	2110 (10)	5175 (13)	67 (26)
(ii) $BaGe_2O_5$ III				
Ba	0	33673 (12)	7885 (8)	74 (2)
Ge(1)	50000	17150 (21)	18228 (13)	66 (4)
Ge(2)	0	0	13995 (14)	80 (4)
O(1)	5000	0	2409 (10)	100 (27)
O(2)	5000	3310 (15)	1004 (9)	73 (25)
O(3)	2500	2500	2500	86 (24)
O(4)	2601 (19)	898 (10)	934 (6)	66 (16)

Experimental. (i) $BaGe_2O_5$ II: parallelogram-plate crystal formed by $\{100\}$, $\{101\}$ and $\{010\}$, volume $0{\cdot}37 \times 10^{-6}$ cm^3; Rigaku automated four-circle diffractometer, graphite-monochromated Ag $K\alpha$ radiation; unit-cell parameters from least-squares fit for 41 reflections with $30 \le 2\theta \le 45°$; integrated intensities measured by 2θ–ω scans; 2746 reflections measured, 2549 independent reflections ($|F_o| > 3\sigma|F_o|$) within

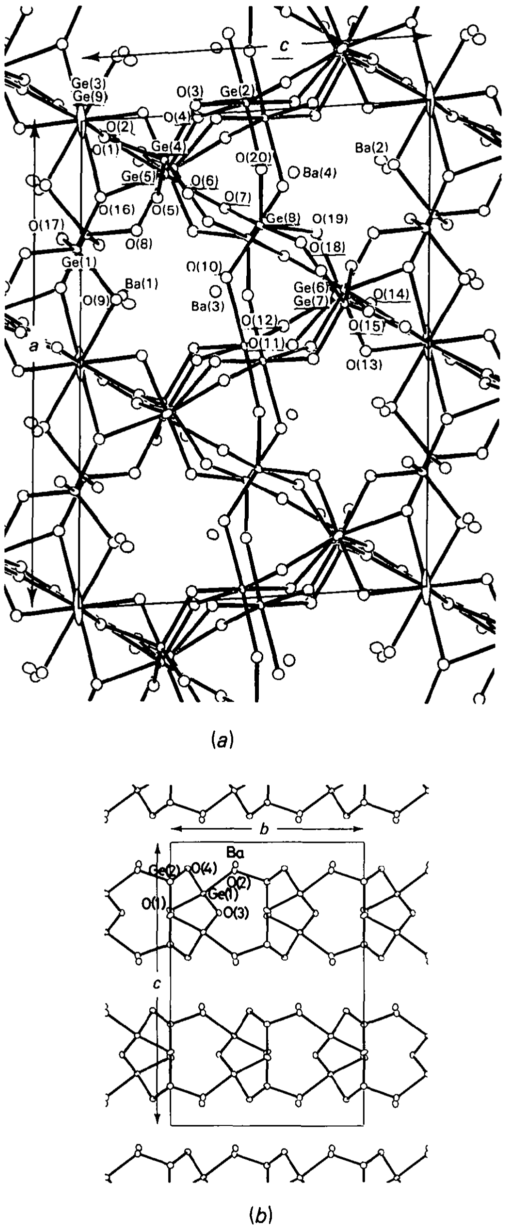

Fig. 1. Projections of (*a*) $BaGe_2O_5$ II along the *b* axis and (*b*) $BaGe_2O_5$ III along the *a* axis. In (*a*) Ba and Ge are represented by their thermal ellipsoids with a probability of 50% and O is represented by a sphere of radius 0·1 Å. In (*b*) all atoms are represented by their thermal ellipsoids with a probability of 50%. Bonds between Ba and O are not drawn.

$0 < 2\theta \le 45°$, 197 unobserved; $(\sin\theta/\lambda)_{\max} = 0{\cdot}682$ Å^{-1}, $0 \le h \le 18$, $0 \le k \le 17$, $-13 \le l \le 13$; four standard reflections every fifty reflections; corrections for Lorentz–polarization and absorption (transmission factor from 0·35–0·59); heavy-atom method; full-matrix least-squares refinement on F using *RADIEL* (Coppens, Guru Row, Leung, Stevens, Becker & Yang, 1979); anisotropic thermal parameters for all atoms; fully ionized scattering factors for Ge^{4+} and Ba^{2+} and f', f'' for Ge, Ba and O from *International Tables for X-ray Crystallography* (1974), scattering factor for O^{2-} from Tokonami (1965); $R = 0{\cdot}047$, $wR = 0{\cdot}049$, $S = 1{\cdot}6080$, $w = 1$; max. $\Delta/\sigma = 0{\cdot}22$; $\Delta\rho$ in final difference map $= -5{\cdot}6$–$+2{\cdot}0$ e Å^{-3}.

Table 2. *Interatomic distances* (Å) *and interbond angles* (°) *with e.s.d.'s in parentheses for* $BaGe_2O_5$ II *and* $BaGe_2O_5$ III

			Distance	*M*–O–*M* angle
(i) $BaGe_2O_5$ II				
Ge(1) tetrahedron				
Ge(1)	–O(9)		1·758(12)	
	–O(8^{ii})		1·764(14)	
	–O(16^{i})		1·789(17)	
	–O(17)		1·717(16)	
O(8^{ii})	–O(9)		2·947(18)	113·56(59)
	–O(16^{i})		2·609(21)	94·48(71)
	–O(17)		2·937(21)	115·04(69)
O(16^{i})	–O(9)		2·938(21)	111·83(68)
	–O(17)		2·929(24)	113·35(76)
O(9)	–O(17)		2·815(20)	108·20(65)
Ge(3) octahedron				
Ge(3)	–O(2)	×2	1·856(14)	
	–O(15^{iv})	×2	1·911(12)	
	–O(9^{iii})	×2	2·003(12)	
O(2)	–O(9^{iii})	×2	2·829(20)	94·23(55)
	–O(15^{iv})	×2	2·494(19)	82·91(56)
	–O(9^{v})	×2	2·628(20)	85·77(55)
	–O(15^{vi})	×2	2·823(18)	97·09(56)
O(15^{vi})	–O(9^{iii})	×2	2·836(18)	92·85(51)
O(15^{iv})	–O(9^{iii})	×2	2·698(17)	87·15(51)
Ge(5) octahedron				
Ge(5)	–O(2)		1·926(14)	
	–O(4)		1·814(15)	
	–O(5)		1·794(14)	
	–O(7)		1·912(13)	
	–O(8)		1·847(14)	
	–O(15^{iv})		2·470(14)	
O(5)	–O(2)		2·779(19)	96·64(60)
	–O(4)		2·829(20)	103·29(65)
	–O(7)		2·725(18)	94·63(58)
	–O(8)		2·568(19)	89·71(62)
O(15^{iv})	–O(2)		2·494(19)	67·82(51)
	–O(4)		3·141(20)	93·02(57)
	–O(7)		3·403(18)	101·12(50)
	–O(8)		2·701(19)	75·93(54)
O(2)	–O(4)		2·628(20)	89·25(62)
	–O(8)		2·764(19)	94·19(60)
O(7)	–O(8)		2·539(19)	84·96(58)
O(4)	–O(7)		2·613(18)	89·03(61)
Ge(7) octahedron				
Ge(7)	–O(6^{iv})		1·927(14)	
	–O(12)		1·841(13)	
	–O(13)		1·882(12)	
	–O(14)		1·887(14)	
	–O(16)		2·075(16)	
	–O(19)		1·859(14)	
O(6^{iv})	–O(12)		2·782(19)	95·13(58)
	–O(13)		2·688(17)	89·77(54)
	–O(16)		2·670(20)	83·63(60)
	–O(19)		2·586(19)	86·16(60)
O(14)	–O(12)		2·799(19)	97·29(60)
	–O(13)		2·739(19)	93·25(56)
	–O(16)		2·673(23)	84·72(61)
	–O(19)		2·655(19)	90·26(62)
O(12)	–O(13)		2·588(17)	88·07(54)
	–O(19)		2·717(20)	94·51(60)
O(13)	–O(16)		2·557(21)	80·36(56)
O(16)	–O(19)		2·949(20)	96·95(62)
Ge(2) octahedron				
Ge(2)	–O(3)		1·868(12)	
	–O(4)		1·920(15)	
	–O(10^{iii})		1·923(12)	
	–O(11^{iii})		1·878(13)	
	–O(12^{iii})		1·886(13)	
	–O(20)		1·900(12)	
O(20)	–O(3)		2·616(17)	87·92(52)
	–O(4)		2·848(19)	96·38(57)
	–O(11^{iii})		2·709(18)	91·61(53)
	–O(12^{iii})		2·626(18)	87·80(54)
O(10^{iii})	–O(3)		2·611(18)	87·06(53)
	–O(4)		2·609(20)	85·52(57)
	–O(11^{iii})		2·769(18)	93·53(54)
	–O(12^{iii})		2·686(18)	89·66(55)
O(3)	–O(4)		2·617(19)	87·38(58)
	–O(12^{iii})		2·540(18)	85·18(56)
O(4)	–O(11^{iii})		2·672(19)	89·43(59)
O(11^{iii})	–O(12^{iii})		2·842(19)	98·07(57)
Ge(4) tetrahedron				
Ge(4)	–O(1)		1·762(12)	
	–O(3)		1·743(13)	
	–O(5)		1·759(14)	
	–O(6)		1·725(13)	
O(1)	–O(3)		2·673(17)	99·40(57)
	–O(5)		2·651(18)	97·71(59)
	–O(6)		3·021(17)	120·12(59)
O(3)	–O(5)		2·958(18)	115·27(61)
	–O(6)		2·868(18)	111·62(61)
O(5)	–O(6)		2·885(19)	111·83(63)
Ge(6) tetrahedron				
Ge(6)	–O(11)		1·788(14)	
	–O(14)		1·767(14)	
	–O(15)		1·722(13)	
	–O(18)		1·740(14)	
O(11)	–O(15)		2·676(19)	99·32(63)
	–O(14)		2·821(19)	105·05(64)
	–O(18)		2·805(20)	105·33(64)
O(14)	–O(15)		2·887(20)	111·65(64)
O(15)	–O(18)		2·928(19)	115·51(65)
O(14)	–O(18)		2·997(19)	117·41(65)
Ge(8) hexahedron				
Ge(8)	–O(7)		1·873(13)	
	–O(10)		1·784(13)	
	–O(18)		2·117(14)	
	–O(19)		1·813(13)	
	–O(20)		1·753(12)	
O(7)	–O(10)		2·820(19)	100·88(58)
	–O(19)		2·652(18)	92·04(58)
	–O(20)		2·756(18)	98·92(56)
O(10)	–O(18)		2·564(20)	81·70(57)
	–O(19)		3·141(19)	121·68(59)
	–O(20)		3·132(18)	124·65(58)
O(18)	–O(19)		2·743(20)	88·19(56)
	–O(20)		2·451(18)	77·98(55)
O(19)	–O(20)		2·895(18)	108·56(58)
Ge(9) octahedron				
Ge(9)	–O(1)	×2	1·793(13)	
	–O(13^{i})	×2	1·827(12)	
	–O(16^{i})	×2	2·269(17)	
O(1)	–O(13^{i})	×2	2·610(18)	92·27(55)
	–O(13^{vi})	×2	2·509(17)	87·73(55)
	–O(16^{i})	×2	2·930(22)	91·57(59)
	–O(16^{vi})	×2	2·853(20)	88·43(59)
O(13^{i})	–O(16^{i})	×2	2·557(21)	76·40(56)
	–O(16^{vi})	×2	3·231(20)	103·60(56)

Table 2 (*cont.*)

			Distance	*M*–*O*–*M* angle
Ba(1) polyhedron				
Ba(1)	–O(5)		2·851(13)	
	–O(8)		2·878(14)	
	–O(9)		3·313(16)	
	–O(10)		2·904(13)	
	–O(14^{xi})		2·843(13)	
	–O(17)		2·732(15)	
	–O(16^{xi})		3·013(18)	
	–O(2^{viii})		2·791(14)	
	–O(3^{viii})		2·783(12)	
	–O(1^{viii})		2·895(12)	
	–O(4^{viii})		2·959(14)	
Ba(3) polyhedron				
Ba(3)	–O(6)		2·797(13)	
	–O(9)		2·754(12)	
	–O(10)		2·881(15)	
	–O(11)		3·135(13)	
	–O(18)		3·158(14)	
	–O(4^{i})		3·702(14)	
	–O(7^{i})		2·660(13)	
	–O(19^{i})		2·798(14)	
	–O(11^{vii})		2·896(13)	
	–O(15^{vii})		3·595(13)	
	–O(4^{viii})		2·648(15)	
Ba(2) polyhedron				
Ba(2)	–O(19)		2·920(14)	
	–O(20)		3·328(13)	
	–O(18)		3·473(15)	
	–O(17^{ix})		2·442(15)	
	–O(9^{iv})		3·140(16)	
	–O(13^{iii})		3·009(12)	
	–O(14^{iii})		2·718(13)	
	–O(11^{iii})		3·077(13)	
	–O(12^{iii})		3·671(13)	
	–O(15^{iii})		3·627(13)	
	–O(1^{ix})		2·843(13)	
	–O(2^{ix})		2·771(14)	
	–O(5^{ix})		3·455(13)	
Ba(4) polyhedron				
Ba(4)	–O(3)		3·723 (12)	
	–O(6)		2·979 (13)	
	–O(17^{ix})		3·733 (16)	
	–O(18)		2·561 (14)	
	–O(20)		2·774 (13)	
	–O(12^{iii})		2·912 (13)	
	–O(13^{iii})		2·721 (12)	
	–O(7^{i})		2·784 (12)	
	–O(8^{i})		2·975 (13)	
	–O(10^{i})		3·658 (15)	
	–O(12^{i})		2·818 (13)	
	–O(3^{x})		2·647 (12)	
(ii) $BaGe_2O_5$ III				
Ge(1) octahedron				
Ge(1)	–O(1)		1·889(6)	
	–O(2)		1·964(14)	
	–O(3)	×2	1·864(1)	
	–O(4)	×2	2·013(10)	
O(1)	–O(3)	×2	2·836(1)	98·13(20)
	–O(4)	×2	2·650(14)	85·50(34)
O(2)	–O(3)	×2	2·677(11)	88·71(41)
	–O(4)	×2	2·732(16)	86·77(49)
O(3)	–O(4)	×2	2·745(8)	90·06(27)
	–O(3^{i})		2·782(0)	96·49(9)
O(4)	–O(4^{i})		2·669 (22)	83·05(39)
Ge(2) tetrahedron				
Ge(2)	–O(1^{ii})		1·707(14)	
	–O(4)	×2	1·823(10)	
	–O(2^{iii})		1·762(14)	
O(1^{ii})	–O(4)	×2	2·918(14)	111·44(56)
	–O(2^{iii})		2·820(17)	108·77(66)
O(4)	–O(4^{vi})		2·894(22)	105·10(45)
	–O(2^{iii})	×2	2·937(16)	110·03(57)
Ba polyhedron				
Ba	–O(1^{iv})		2·825(11)	
	–O(2)	×2	2·799(1)	
	–O(2^{v})		3·055(13)	
	–O(3)	×2	2·946(1)	
	–O(4)	×2	2·843(10)	
	–O(4^{vii})	×2	2·898(9)	
	–O(4^{iv})	×2	2·839(10)	

Symmetry code for $BaGe_2O_5$ II

(i)	$0{\cdot}5 - x$,	$-0{\cdot}5 + y$,	$1{\cdot}0 - z$
(ii)	$0{\cdot}5 - x$,	$-0{\cdot}5 + y$,	$-z$
(iii)	$-0{\cdot}5 + x$,	$0{\cdot}5 - y$,	$+z$
(iv)	$0{\cdot}5 - x$,	$0{\cdot}5 + y$,	$1{\cdot}0 - z$
(v)	$0{\cdot}5 - x$,	$0{\cdot}5 + y$,	$-z$
(vi)	$-0{\cdot}5 + x$,	$0{\cdot}5 - y$,	$-1{\cdot}0 + z$
(vii)	$1{\cdot}0 - x$,	$-y$,	$1{\cdot}0 - z$
(viii)	$0{\cdot}5 + x$,	$0{\cdot}5 - y$,	$+z$
(ix)	$+x$,	$+y$,	$1{\cdot}0 + z$
(x)	$-x$,	$-y$,	$1{\cdot}0 - z$
(xi)	$+x$,	$+y$,	$-1{\cdot}0 + z$

Symmetry code for $BaGe_2O_5$ III

(i)	$1{\cdot}0 - x$,	$+y$,	$+z$
(ii)	$-0{\cdot}5 + x$,	$+y$,	$0{\cdot}5 - z$
(iii)	$0{\cdot}5 - x$,	$-0{\cdot}5 + y$,	$+z$
(iv)	$0{\cdot}5 - x$,	$0{\cdot}5 + y$,	$+z$
(v)	$-0{\cdot}5 + x$,	$0{\cdot}5 - y$,	$-z$
(vi)	$-x$,	$+y$,	$+z$
(vii)	$0{\cdot}5 - x$,	$0{\cdot}5 - y$,	$-z$

(ii) $BaGe_2O_5$ III: tetragonal columnar crystal formed by {100}, {010} and {001}, volume $0{\cdot}104 \times 10^{-6}$ cm^3; unit-cell parameters from least-squares fit for 35 reflections with $30 \le 2\theta \le 45°$; 776 reflections measured, 535 independent reflections ($|F_o| > 2\sigma|F_o|$) within $0 < 2\theta \le 50°$, 241 unobserved; $(\sin\theta/\lambda)_{\max} = 0{\cdot}7535$ Å^{-1}, $0 \le h \le 8$, $0 \le k \le 14$, $0 \le l \le 21$; $R = 0{\cdot}051$, $wR = 0{\cdot}064$, $S = 2{\cdot}314$, $w = 1$; max. $\Delta/\sigma = 0{\cdot}29$; $\Delta\rho$ in final difference map $= -3{\cdot}7$–$+2{\cdot}3$ e Å^{-3}. All other data as for (i).

Discussion. Final atomic parameters are given in Table 1.* The *ORTEP* plots of the structure of $BaGe_2O_5$ II

---

* Lists of structure factors and anisotropic thermal parameters have been deposited with the British Library Lending Division as Supplementary Publication No. SUP 42127 (26 pp.). Copies may be obtained through The Executive Secretary, International Union of Crystallography, 5 Abbey square, Chester CH1 2HU, England.

and $BaGe_2O_5$ III are shown in Fig. 1 (Johnson, 1965). In Table 2, bond distances and bond angles are listed.

(i) $BaGe_2O_5$ II: Ge tetrahedra [Ge(1), Ge(4), Ge(6)], Ge hexahedra [trigonal bipyramids, Ge(8)] and Ge octahedra [Ge(2), Ge(3), Ge(5), Ge(7), Ge(9)] constitute the framework of the structure. The mean coordination of Ge is 5·125. There are three kinds of infinite chains of Ge polyhedra; two are parallel to the *a* axis [Ge(9), Ge(1), Ge(3), Ge(1), Ge(9) polyhedra; Ge(2), Ge(8), Ge(2), Ge(8), Ge(2) polyhedra], and the other one is parallel to the *b* axis [Ge(7), Ge(4), Ge(5), Ge(6), Ge(7) polyhedra]. These three chains form two ladder-like sheets, one parallel to (201) and the other to ($\bar{2}01$). These are shown in Fig. 2. As shown in Fig. 1(*a*), this configuration of Ge polyhedra forms big tunnels along the *b* axis, where the Ba are located. As is seen in Table 2, the distances between Ba and the ambient oxygens are widely ranged, so that it is difficult to determine the coordination number for the four Ba. However, it seems to be around 11. As shown in Fig. 2(*c*), Ge(3) and Ge(5) octahedra share an edge, and Ge(7) and Ge(9) octahedra also. As seen in Table 2, the distances Ge(5)—O(15) and Ge(9)—O(16) are extraordinarily long, and these Ge(5) and Ge(9) octahedra are largely distorted. The fact that both O(15) and O(16) are shared by three Ge polyhedra [Ge(5) and Ge(3) octahedra and Ge(6) tetrahedron for O(15), Ge(9) and Ge(7) octahedra and Ge(1) tetrahedra for O(16)] might be related to these distortions.

(ii) $BaGe_2O_5$ III: Ge tetrahedra and Ge octahedra constitute a double-sheet structure. The mean coordination number of Ge is 5·0. As shown in Fig. 1(*b*), the sheet is perpendicular to the *c* axis. This structure is similar to that of the hexagonal perovskite-like compounds ABX_3 at high pressures (Syono, Akimoto & Kohn, 1969). That is, a view of this structure along the *c* axis shows that it is composed of layers consisting of O and Ba parallel to (001). The stacking of the layers is represented by the repetition –Ba·3O–4O–Ba·3O–Ba·3O–4O–Ba·3O–, forming a hexagonally close-packed structure. The coordination number of Ba is 12 and Ge occupy tetrahedral and octahedral interstices, which are possible only between Ba·3O and 4O layers and there is neither edge sharing nor face sharing of Ge polyhedra. As shown in Table 2, Ge and Ba polyhedra are not distorted. This very regular h.c.p. structure resulted in a higher density (6·12 g cm^{-3}).

Increase in density from II to III is 4·4%, which could be explained by the increase in coordination number of Ba, while the coordination number of Ge decreased slightly.

Large electron densities are found in the final difference map for both phases ($\pm\Delta\rho \simeq 3$ e Å^{-3}). A similar residue is also observed in the case of another phase in the system BaO–GeO_2 (Ozima, 1985). This seems to be due to the inadequate fully ionized ionic model (Ba^{2+}, Ge^{4+}, O^{2-}) for these substances.

The author thanks Dr T. Kobayashi and Professor Y. Shimizu of Meiji University who kindly provided her with single crystals of $BaGe_2O_5$ III.

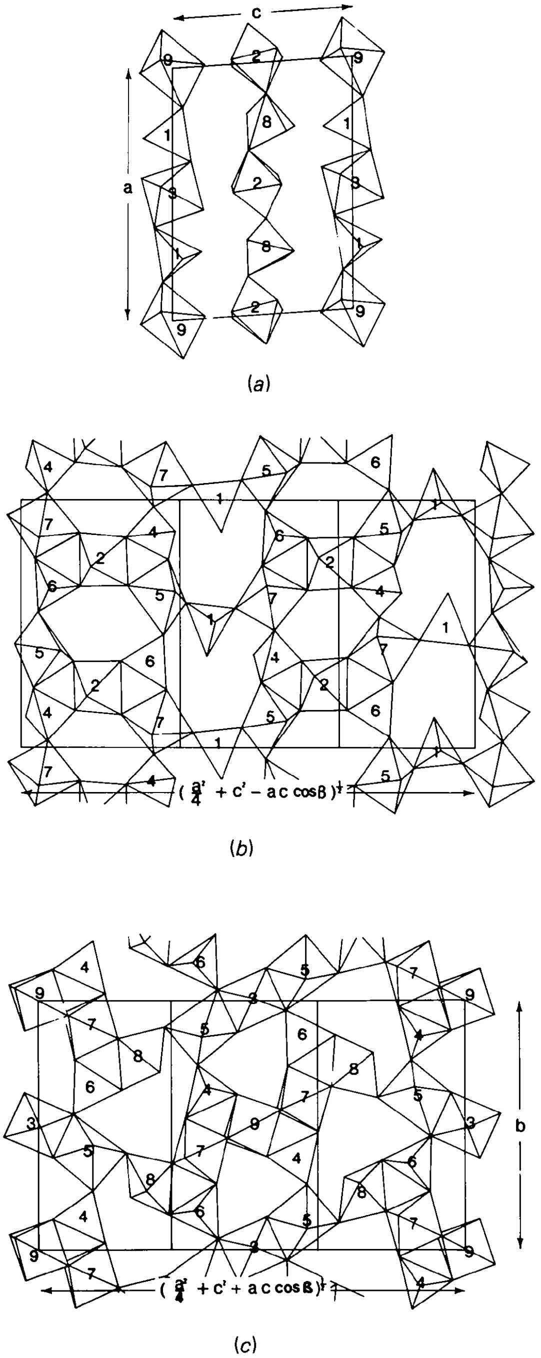

Fig. 2. Linkages of polyhedra in (*a*) chains along the *a* axis, (*b*) a sheet parallel to (201), and in (*c*) a sheet parallel to ($\bar{2}01$) of $BaGe_2O_5$ II.

References

Coppens, P., Guru Row, T. N., Leung, P., Stevens, E. D., Becker, P. J. & Yang, Y. W. (1979). *Acta Cryst.* A**35**, 63–72.

International Tables for X-ray Crystallography (1974). Vol. IV. Birmingham: Kynoch Press. (Present distributor D. Reidel, Dordrecht.)

Johnson, C. K. (1965). *ORTEP*. Report ORNL-3794. Oak Ridge National Laboratory, Tennessee.

Katscher, H., Bissert, G. & Liebau, F. (1973). *Z. Kristallogr.* **137**, 146–158.

Kobayashi, T., Ozima, M., Shimizu, Y. & Akimoto, S. (1983). Program and Abstracts, 24th High-Pressure Conference of Japan, p. 192.

Natl Bur. Stand. (*US*) *Monogr.* (1976). No. 25, p. 10.

Ozima, M. (1985). In preparation.

Ozima, M., Susaki, J., Akimoto, S. & Shimizu, Y. (1982). *J. Solid State Chem.* **44**, 307–317.

Syono, Y., Akimoto, S. & Kohn, K. (1969). *J. Phys. Soc. Jpn*, **26**, 993–999.

Tokonami, M. (1965). *Acta Cryst.* **19**, 486.

Acta Cryst. (1985). C**41**, 1007–1009

Structure of $MnIn_2Te_4$-II, an Indium Manganese Telluride High-Pressure Phase

By Beate Panzer and Klaus-Jürgen Range*

Institute of Inorganic Chemistry, University of Regensburg, Universitätsstrasse 31, *D*-8400 *Regensburg, Federal Republic of Germany*

(*Received* 15 *October* 1984; *accepted* 18 *March* 1985)

Abstract. $M_r = 794{\cdot}978$, orthorhombic, $Pnma$, $a = 28{\cdot}279\,(3)$, $b = 4{\cdot}376\,(2)$, $c = 7{\cdot}124\,(2)$ Å, $V = 881{\cdot}59$ Å^3, $Z = 4$, $D_x = 5{\cdot}989$ Mg m^{-3}, Mo $K\alpha$, $\lambda = 0{\cdot}7107$ Å (graphite monochromator), $\mu = 199{\cdot}64$ mm^{-1}, $F(000) = 1292$, $T = 296$ K, final $R = 0{\cdot}0267$ for 853 unique reflections. The high-pressure phase $MnIn_2Te_4$-II has been synthesized from $MnIn_2Te_4$-I at a hydrostatic pressure of 1·5 GPa and $T = 1073$ K. The structure comprises layers of $MnTe_6$ octahedra [Mn–Te 2·889 (2)–3·014 (2) Å] stacked along [100] and bridged by chains of $InTe_4$ tetrahedra [In(1)–Te 2·767 (1)–2·794 (1); In(2)–Te 2·756 (1)–2·835 (1) Å].

Introduction. The structure of $MnIn_2Te_4$-I (tetragonal, space group $I\bar{4}2m$, $a = 6{\cdot}191$, $c = 12{\cdot}382$ Å), stable at atmospheric pressure, can be derived from the sphalerite structure (Range & Hübner, 1975). The doubling of one of the three cubic axes of the sphalerite-type unit cell is caused by an ordering of the vacancies as in the $CdGa_2S_4$- and β-Cu_2HgI_4-type structures. However, the different cations are distributed randomly over the occupied tetrahedral sites. The purpose of this study was to achieve an ordered arrangement of the different cations under the influence of high pressure.

Experimental. Experiments were carried out in a modified Belt-type high-pressure apparatus (Range & Leeb, 1975) using BN as crucible material. Temperature was varied in the range 973 to 1173 K, pressure in the range 0·5 to 2·0 GPa. Up to 1·0 GPa and 1073 K the phase $MnIn_2Te_4$-I remains stable. After quenching from 1·5 GPa and 1073 K a new phase was obtained, and proved to be homogeneous by Guinier photographs. Therefore, this phase ($MnIn_2Te_4$-II) is a high-pressure phase, metastable under normal conditions. At still higher temperatures and pressures $MnIn_2Te_4$-II becomes unstable again and decomposes.

A silvery crystal fragment (approx. 20 × 30 × 60 μm) used for data collection on an Enraf–Nonius CAD-4 diffractometer; 25 reflections used for measuring lattice parameters; experimental absorption correction (ψ scan, min. correction factor 0·9511, max. 0·9994); intensities measured for $2° < \theta < 25°$; ω–2θ scan technique; $0 \le h \le 33$, $-5 \le k \le 5$, $-8 \le l \le 8$; three standard reflections ($\bar{2}00$, $\bar{1}1\bar{4}$, $\bar{3},0,\bar{12}$) with a total loss of intensity of 3% throughout data collection; 3149 reflections measured, 853 unique ($R_{\rm int} = 0{\cdot}03$), 210 unobserved [$F < 2\sigma(F)$]. The positional parameters of the first four Te atoms [Te(1)] were determined using direct methods (*MULTAN*82; Main, Fiske, Hull, Lessinger, Germain, Declercq & Woolfson, 1982); the positions of the remaining Te atoms and of the cations were taken from difference Fourier syntheses (*SHELX*76; Sheldrick, 1976). In least-squares refinement $|F|$ magnitudes were used to refine atomic coordinates, occupation factors and anisotropic temperature factors. $R = 0{\cdot}0267$, $wR = 0{\cdot}0356$ [$w = k/\sigma(F)^2 + |g|F^2$]. $(\Delta/\sigma)_{\max} < 0{\cdot}001$ in final refinement cycle. Final difference Fourier synthesis showed residual electron density of 1·14 (max.) and −2·11 e Å^{-3} (min.). Atomic scattering factors and f', f'' values from *International Tables for X-ray Crystallography* (1974). Bond distances and angles calculated using the program *SADIAN* (Baur & Wenninger, 1969).

---

* To whom correspondence should be addressed.

0108-2701/85/071007-03$01.50